New Zealand Journal of Geology & Geophysics, 2005, Vol. 48: 229–245
0028–8306/05/4802–0229 © The Royal Society of New Zealand 2005

The Paleozoic–Mesozoic recycling of the Rakaia Terrane, South Island, New Zealand: sandstone clast and sandstone petrology, geochemistry, and geochronology

ANEKANT M. WANDRES
JOHN D. BRADSHAW
Department of Geological Sciences
University of Canterbury
Private Bag 4800
Christchurch, New Zealand
anekant.wandres@canterbury.ac.nz

TREVOR IRELAND
Geochronology and Isotope Geochemistry
Research School of Earth Sciences
The Australian National University
Canberra ACT 0200, Australia

Abstract The Torlesse terranes—part of the New Zealand Eastern Province—are accretionary complexes that comprise an enormous volume of quartzofeldspathic sandstones and mudstones with subsidiary conglomerates plus minor oceanic assemblages. Two terranes are recognised in the South Island—the Permian to Late Triassic Rakaia Terrane and the Late Jurassic to Early Cretaceous Pahau Terrane. Sandstone clasts from two Rakaia Terrane and two Pahau Terrane conglomerates were collected. We present the first combined detailed information on petrography and geochemistry of Torlesse conglomerate sandstone clasts and use our own and published U-Pb SHRIMP detrital zircon age data to demonstrate the recycling of the Rakaia Terrane into Rakaia strata itself and into Pahau Terrane strata.

Sandstone clast major and trace element chemical data largely support petrographic observations derived from thin-section analysis. The similarities of petrographic and geochemical data between sandstone clasts from the Rakaia Terrane and Rakaia sandstones suggest that clasts in the Permian Te Moana and Late Triassic Lake Hill Conglomerates were derived by autocannibalistic reworking of older, consolidated, Rakaia sediments. Data from sandstone clasts from the Pahau Terrane suggest that uplift of the Rakaia Terrane continued into the Cretaceous. These Pahau Terrane clasts indicate that at the time of the Pahau sedimentation Permian to early Late Triassic Rakaia rocks were exposed and recycled into the Pahau Basin.

Keywords sandstone; provenance; Terrane recycling; petrography; geochemistry; zircon; geochronology; Pahau Terrane; Rakaia Terrane; Gondwana margin

G03067; Online publication date 25 May 2005
Received 3 November 2003; accepted 13 July 2004

INTRODUCTION

Sandstones and mudstones of the Late Permian to Early Cretaceous Torlesse Supergroup underlie c. 60–70% of the New Zealand land area and a large part of the New Zealand micro-continent. In the South Island, Torlesse sediments are divided in two terranes—the Permian to Late Triassic Rakaia Terrane and the Late Jurassic to Early Cretaceous Pahau Terrane (Fig. 1). These two terranes are separated by the Esk Head Melange (Bradshaw 1973; Silberling et al. 1988). Recent studies of Torlesse depositional and deformational environments favour a submarine fan depositional model and an accretionary wedge deformational model for the Torlesse rocks (Howell 1980; Bradshaw et al. 1981; George 1992; Mazengarb & Harris 1994).

The provenance of the Torlesse terranes has occupied New Zealand geologists for many years (Andrews et al. 1976; Coombs et al. 1976; Howell 1980; MacKinnon 1983; Korsch & Wellman 1988; Bradshaw 1989; Mortimer 1995; Roser & Korsch 1999). Sandstone petrography, sedimentary geochemistry, detrital mineral geochronology, and isotope geochemical studies of sediments have all been employed to address this problem (e.g., MacKinnon 1983; Roser 1986; Roser & Korsch 1988, 1999; Frost & Coombs 1989; Ireland 1992; Mortimer 1995; Adams & Graham 1996; Cawood et al. 1999, 2002; Pickard et al. 2000). These studies have broadly established a mixed cratonic arc provenance, but on their own they are incapable of establishing a specific source. Various sediment sources have been proposed, including a provenance east of present-day New Zealand (Andrews et al. 1976), Marie Byrd Land in Antarctica (Korsch & Wellman 1988; Wandres et al. 2004a), and the New England Fold Belt in eastern Australia (Adams & Kelley 1998; Pickard et al. 2000). More local sources have also been proposed for the younger Pahau Terrane, such as the older Rakaia Terrane (MacKinnon 1983; Smale 1997; Roser & Korsch 1999; Leverenz & Ballance 2001; Wandres et al. 2004b). However, Adams & Graham (1996) concluded that initial $^{87}Sr/^{86}Sr$ ratios of the younger Pahau Terrane at the time of metamorphism are inconsistent with the Rakaia Terrane being a dominant sediment source for the Pahau Terrane.

Only a few authors have given detailed geologic and petrographic descriptions of sandstone clasts from Torlesse conglomerates (Andrews et al. 1976; Smale 1978, 1980, 1983; MacKinnon 1983; Barnes 1990; Leverenz & Ballance 2001). They noted an abundance of Torlesse-like sandstone clasts, which were inferred to have been reworked from older Torlesse rocks. MacKinnon (1980) studied thin sections from 17 pebble-sized conglomerates and showed that most sandstone clasts are indistinguishable from coeval or older Torlesse sandstones. MacKinnon showed that sandstone clasts, together with mudstone clasts of similar composition, compose c. 10–30% of the clasts in Permian and some Middle Triassic Torlesse conglomerates, and 50% or more in some Middle Triassic and most younger Torlesse conglomerates. Smale (1983) described petrographic similarities between

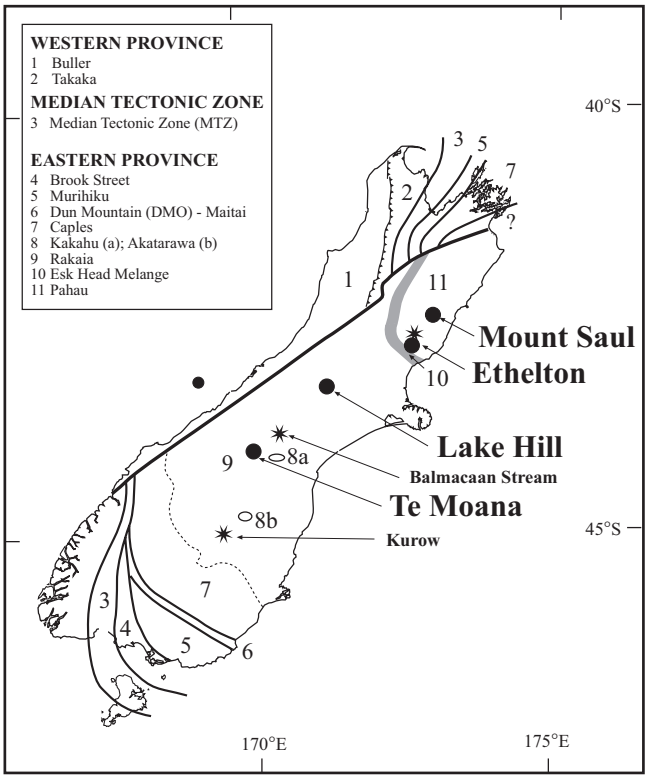

Fig. 1 Tectonostratigraphic terrane map of New Zealand showing distribution of conglomerate locations (filled circles). Also shown are localities of sandstone samples used for U-Pb zircon age (SHRIMP) determination (stars). Terrane affiliation of Marlborough Schist (shown as ?) uncertain.

sandstone clasts, conglomerate matrix, and interbedded sandstones in the Permian Te Moana Conglomerate. He concluded that the conglomerate matrix was derived from the sandy substrate and that the sources of the sandstone and the sandstone clasts were the same. MacKinnon (1980) noted that the matrix of all the conglomerates is medium to coarse grained, and that in pre-Jurassic conglomerates the composition of matrix is different from that which would be produced by simple breakdown of conglomerate clasts; thus, matrix and clasts were derived in part from different sources. In Upper Jurassic and Lower Cretaceous conglomerates, composition of matrix and clasts is compatible with the derivation from the same source.

We present the first combined detailed information on petrography and geochemistry of Torlesse conglomerate sandstone clasts and use our own and published U-Pb SHRIMP detrital zircon age data to demonstrate how and when the Rakaia Terrane rocks have been recycled. This paper complements the Rakaia and Pahau Terrane provenance study using igneous conglomerate (Wandres & Bradshaw 2005; Wandres et al. 2004a,b).

Conglomerate clast lithologies

Conglomerates are rare and constitute <1% of the Torlesse terranes. Although excellently preserved stratigraphic sections up to a few hundred metres thick are widespread, there is a general lack of marker beds and a common occurrence of zones of pervasive tectonic disruption. In addition, isoclinal folding and tectonic imbrication is pervasive throughout the Torlesse Terrane, and stratigraphic control is poor.

In general, the four Torlesse conglomerates at Te Moana (Permian depositional age, grid ref. NZMS 260 J37/488880), Lake Hill (Late Triassic: Carnian; K35/955605), Ethelton (Early Cretaceous: Barremian; N33/127149), and Mount Saul (Aptian; M32/865445) are dominated by beds of poorly to moderately sorted, matrix/clast-supported conglomerates interbedded with massive to thinly bedded, often graded sandstones. A quartzose sandstone matrix predominates in the conglomerates but silt matrix occurs, especially in matrix-supported conglomerate beds. Most clasts are rounded to well rounded with a clast-supported framework, but may grade into matrix-supported units. All clasts are indurated to well indurated. Clast sizes range from pebble to boulder size, with a variable average grain size ranging from 20 to 60 mm. Clast populations in all conglomerates are dominated by sandstones and volcanics. Overall, five lithological groups are distinguished: (1) arenites 29–60%; (2) volcanics 5–41%; (3) granitoids 7–23%; (4) lutites 11–15%, and (5) others including quartz and chert 7–14%.

Sandstones

Sandstone samples from two Rakaia Terrane localities (Kurow, Balmacaan; Fig. 1) and a matrix sample of the Ethelton conglomerate were collected for zircon U-Pb ages analyses. The sample from Kurow is a dark grey, bedded, medium–coarse-grained sandstone with a weak foliation and was collected from the slope of Kurow Hill (I40/093060) just to the north of Kurow. *Atomodesma* (Permian) fragments were reported from the same hill by Campbell & Warren (1965). The Balmaccan Stream sample is a dark grey to grey and fine–medium-grained sandstone that was collected from an exposure in the river bank of the Balmacaan Stream (J36/518283). Van Dusschoten (1998) reported the first known Anisian fossils (NZFR J36/f99, *Trigonia balmae*, *Mellarium nodulosum*, *Parapopanoceras fraseri*, and *Daonella jadii*) in the Rakaia Terrane from the Balmacaan Stream area. The sample from the conglomerate matrix at Ethelton is from a massive, grey-brown, medium grained sandstone bed. The conglomerate contains a mixed Late Jurassic to Early Cretaceous dinoflagellate assemblage (Campbell & Warren 1965).

SAMPLES AND ANALYTICAL METHODS

Fifty sandstone clasts were collected from two Rakaia Terrane (Te Moana, $n = 14$; Lake Hill, $n = 12$) and two Pahau Terrane (Mount Saul, $n = 12$; Ethelton, $n = 12$) conglomerates. Criteria for sampling were: rip-up conglomerate clasts (derived from erosion of semi-consolidated sediments) and highly silicified clasts were excluded, degree of alteration, and size (c. 10 cm).

Sandstone petrographic modes were determined by point counting 500 grains in stained thin sections using the standard Gazzi-Dickinson method, providing modes considered accurate to within 5% of true values (Van Der Plas & Tobi 1965). Petrographic procedures and sandstone classification followed MacKinnon (1983). Detrital categories include quartz, plagioclase, potassium feldspar, various rock fragments, mafic mineral categories, and matrix (Table 1). Accurate determination of the original detrital mineralogy of a sandstone can only be accomplished if the sample has little alteration, so considerable care was taken to select

Table 1 Composition of Torlesse sandstone clasts from four conglomerate locations. Q = framework quartz, F = feldspar, L = lithic fragments; contents have been recalculated to 100%; P/F = plagioclase to total feldspar ratio; Lv/L = volcanic lithic fragment to total lithic fragment ratio; %M = framework percent mica. Alterites are detrital framework grains altered beyond recognition. Point counts were of a minimum of 500 grains. Procedures, definitions of parameters, and grain types follow MacKinnon (1980), who, with one minor exception, followed Dickinson (1970). MacKinnon counted rare phenocrysts within aphanitic rock fragments as rock fragment rather than as phenocryst minerals.

No. of samples:	All samples $n = 50$				Te Moana $n = 14$				Lake Hill $n = 12$				Ethelton $n = 12$				Mount Saul $n = 12$			
	Min.	Max.	Mean	CI	Min.	Max.	Mean	CI	Min.	Max.	Mean	CI	Min.	Max.	Mean	CI	Min.	Max.	Mean	CI
Size	0.20	0.45	0.30		0.25	0.45	0.31		0.20	0.45	0.31		0.20	0.40	0.28		0.25	0.45	0.32	
Quartz	13	40	22		17	26	21		13	25	20		14	40	22		24	28	26	
Polyquartz + chert	0	6	2		0	2	1		1	6	3		1	6	3		1	4	2	
Potassium feldspar	4	21	12		7	14	10		8	18	13		4	17	10		10	18	14	
Plagioclase	19	37	28		27	37	32		19	32	27		22	35	29		22	29	25	
Volcanic lithics	6	25	12		11	21	14		11	25	14		6	22	11		7	16	10	
Metamorphic lithics	0	4	1		0	2	1		1	4	2		0	2	1		1	2	1	
Sedimentary lithics	0	8	4		2	8	5		2	6	4		0	6	3		1	6	3	
Mica	2	8	5		3	6	4		3	5	4		2	7	5		3	8	6	
Heavy minerals	1	7	4		2	6	3		2	5	4		1	6	4		3	7	5	
Others (cement + alterite)	0	1	1		0	1	1		0	1	1		1	1	1		0	1	1	
Matrix	4	14	9		7	10	9		6	11	9		5	14	11		4	9	7	
Q			30.1	1.6			26.3	1.6			28.1	2.4			31.7	4.9			34.6	1.1
F			48.9	1.2			50.1	1.9			48.0	2.4			48.9	3.4			48.0	2.6
L			21.0	1.7			23.7	1.7			23.9	3.0			19.4	5.1			17.4	2.5
P/F			0.70	0.02			0.76	0.03			0.68	0.05			0.75	0.06			0.64	0.03
Lv/L			0.71	0.02			0.71	0.05			0.72	0.04			0.71	0.07			0.70	0.03
%M			5.40	0.49			5.11	0.72			4.08	0.50			5.86	1.14			6.51	1.17

Fig. 2 **A**, QFL diagram for sandstone clasts from the four conglomerate locations at Te Moana (n = 14), Lake Hill (n = 12), Ethelton (n = 12), and Mount Saul (n = 12). Also plotted are sandstone clasts from MacKinnon (1980). **B**, Mean values for the four sandstone clast populations compared with the five Torlesse sandstone petrofacies (PF1–5) of MacKinnon (1980, 1983). All hexagonal boxes around mean compositions are 95% confidence intervals. Dotted line with arrow shows the evolution trend of the Torlesse sandstone of MacKinnon (1983).

samples which have experienced only minimal diagenetic and weathering modifications after deposition. Heavily veined samples were not counted. When point counting, incomplete alteration of grains or pseudomorphs, such as sericitised or albitised plagioclase or chloritised biotite, was ignored if it did not prevent recognition of original detrital grain composition. The remaining alteration or replacement components fall into the categories "matrix" or "others", which includes "alterites" and "cement". The average and range of these, for the samples selected, are: matrix 9% (4–14%); others <1% (0–1.4%) (Table 1). Quartz and feldspar crystals >0.0625 mm within microphaneritic lithic fragments are reapportioned to the quartz and feldspar categories. This was suggested by Dickinson (1970) and follows MacKinnon's procedures. In the same manner, perthitic, granophyric, and micrographic grains were also reapportioned. Hence, there are no plutonic or gneissic lithic fragment categories. Polycrystalline quartz and sedimentary, metamorphic, and volcanic fragments are categorised as lithic fragments. Contrary to Dickinson's

(1970) suggestion, phenocrysts in aphanitic lithic fragments were counted as part of the lithic fragment (MacKinnon 1980). A few sandstones contain mudstone rip-up clasts, which were clearly recognisable by their large size. They were not included in the point counts.

Major and trace element compositions were determined from the 50 samples by X-ray fluorescence (XRF) at the University of Canterbury, following Weaver et al. (1990). All elemental concentrations have been renormalised to 100% anhydrous.

U-Pb crystallisation ages of detrital zircons of Rakaia and Pahau sandstones were obtained on SHRIMP RG and SHRIMP I at Stanford University in California and at the Australian National University, Canberra. Methods are described in detail by Muir et al. (1997). The ANU standard SL13 was used to normalise the U concentration (238 ppm); the Th concentration was then derived from the Th/U ratio. Duluth standards AS3 and FC1 were used to calibrate U/Pb ratios after correction of Pb^+/U^+ for correlated variation with UO^+/U^+. The Temora standard (417 Ma) was included in one mount as a secondary standard. The zircons are dominated by Phanerozoic material, so emphasis was placed on determining the $^{206}Pb/^{238}U$ age. For zircons younger than c. 800 Ma, $^{207}Pb/^{206}Pb$ of individual zircons is an insensitive chronometer, and determination of concordance to any degree of resolution is not practical. To this end, ^{204}Pb and background were not collected, allowing the data to be collected in a substantially reduced period compared with the full analysis optimising ^{204}Pb, background, and ^{207}Pb. The few older zircons with Proterozoic ages must be regarded as suspect, but the issue with this age range is to establish the presence of a general age component rather than determine the exact geochronology. Detailed descriptions and geochemistry of individual sandstone clasts are available on request from the authors. The AGSO Phanerozoic Time Scale (Jones 1995) is used.

Table 2 Average compositions of sandstone clasts from four conglomerate locations (volatile free normalised basis).

No. of samples:	Te Moana $n = 14$		Lake Hill $n = 12$		Ethelton $n = 12$		Mount Saul $n = 12$	
	Mean	95CI	Mean	95CI	Mean	95CI	Mean	95CI
SiO_2	71.06	0.88	71.22	1.16	70.84	3.10	74.36	1.18
TiO_2	0.53	0.04	0.54	0.08	0.53	0.09	0.41	0.05
Al_2O_3	14.78	0.25	14.50	0.45	14.52	1.25	13.51	0.45
Fe_2O_{3T}	3.86	0.53	4.07	0.53	3.89	0.73	2.96	0.37
MnO	0.05	0.01	0.06	0.01	0.06	0.01	0.04	0.01
MgO	1.13	0.14	1.27	0.21	1.34	0.37	0.93	0.13
CaO	2.19	0.15	1.61	0.34	1.98	0.51	1.13	0.23
Na_2O	4.05	0.13	4.22	0.20	4.09	0.38	3.62	0.16
K_2O	2.23	0.22	2.42	0.22	2.62	0.30	2.95	0.15
P_2O_5	0.13	0.01	0.12	0.02	0.12	0.03	0.10	0.01
SiO_2/Al_2O_3	4.81	0.14	4.93	0.22	5.07	0.88	5.53	0.26
K_2O/Na_2O	0.56	0.07	0.58	0.06	0.66	0.09	0.82	0.07
CIA	53.73	0.57	54.35	0.63	53.10	0.69	55.21	0.77
Ba (ppm)	638	46	613	79	685	139	674	46
Ce	63	3	70	5	59	5	58	6
Cr	27	2	32	10	28	6	33	5
Cu	10	1	10	1	11	3	8	1
Ga	16	1	16	1	16	2	15	1
La	28	2	29	3	23	3	26	3
Nb	10	1	10	1	9	1	9	1
Nd	31	3	32	4	28	4	25	4
Ni	10	1	14	3	10	2	12	2
Pb	18	1	20	3	14	2	19	1
Rb	70	7	86	8	86	10	105	7
Sc	10	1	11	2	10	2	8	1
Sr	341	15	314	45	320	72	288	44
Th	13	2	12	2	9	1	12	1
U	4	0	4	0	4	0	4	0
V	73	7	74	11	75	17	60	10
Y	23	1	25	2	21	2	21	2
Zn	55	5	54	7	56	10	44	6
Zr	238	27	209	15	197	20	192	25
Th/Sc	1.3	0.1	1.2	0.2	1.0	0.2	1.5	0.2
La/Sc	2.8	0.3	2.7	0.4	2.6	0.7	3.2	0.5
Ce/Sc	6.3	0.5	6.6	0.9	6.5	1.3	7.5	1.2
Zr/Sc	23.7	2.7	19.5	2.2	21.8	4.6	24.1	3.0
La_N/Y_N	7.0	0.6	6.6	0.7	6.3	1.0	7.2	0.9
V/La	2.6	0.4	2.6	0.5	3.5	1.1	2.4	0.4
Ti/Zr	13.5	0.7	15.5	2.2	16.2	2.8	12.9	1.1
F1	0.88	0.89	0.13	0.34	–0.18	0.97	–1.85	0.45
F2	2.24	0.76	2.31	0.61	2.53	0.70	2.49	0.24

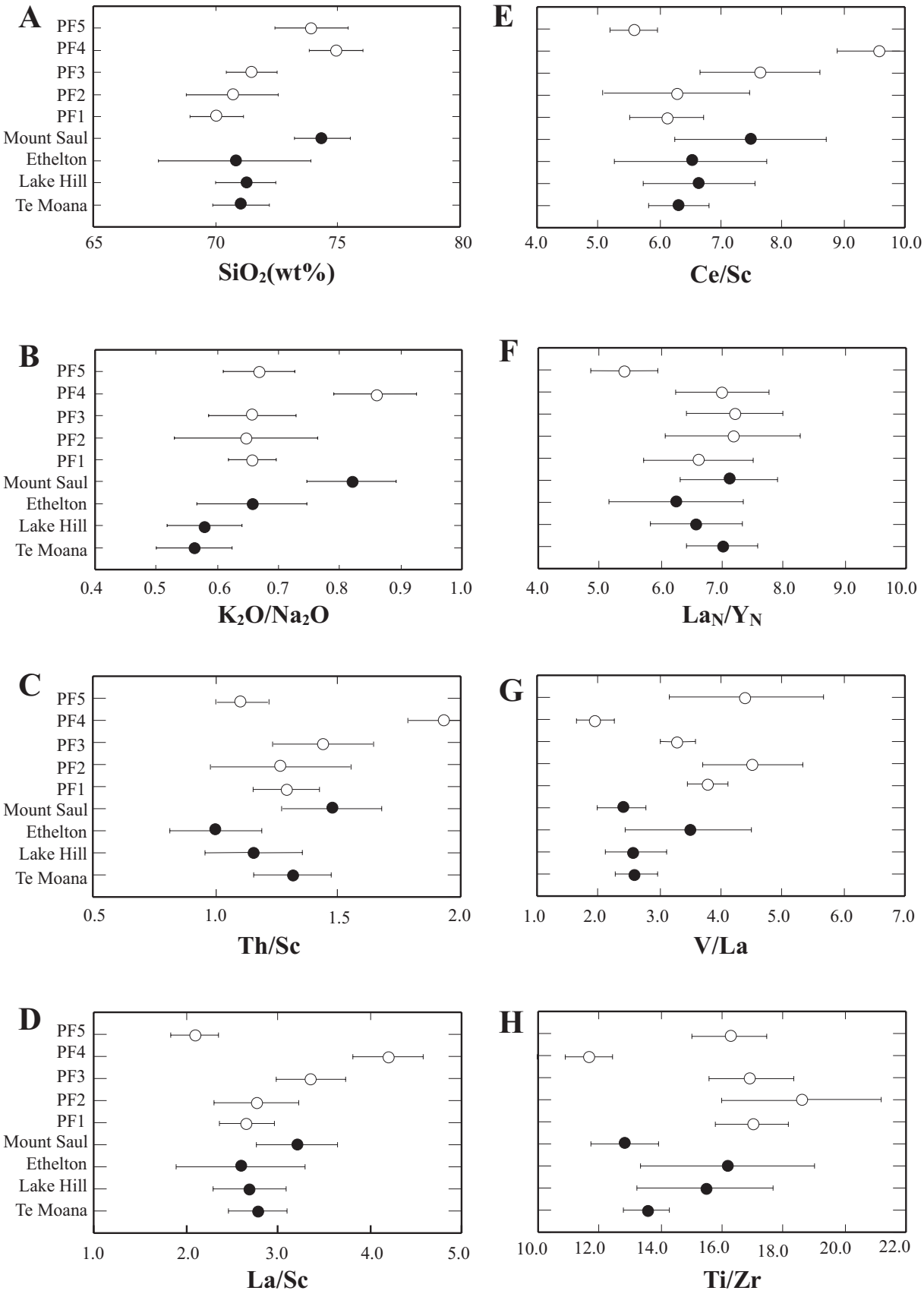

Fig. 3 A–H Mean geochemical values for the Te Moana (n = 14), Lake Hill (n = 12), Ethelton (n = 12), and Mount Saul (n = 12) sandstone clast populations (filled circles) are compared to mean values (open circles) of the five sandstone petrofacies from Roser et al. (1995) and Roser & Korsch (1999). Bars represent 95% confidence intervals. **A, B**, Values for major elements. **C–H**, Values for trace element ratios.

RESULTS

Petrographic composition of sandstone clasts

Sandstone clasts from each conglomerate were distinguished on the basis of compositional parameters determined in the point counts (Table 1).

QFL are the major components and are shown in Fig. 2A together with the five sandstone petrofacies (PF) defined by MacKinnon (1980). The following are average framework compositions for the four Rakaia PFs: $Q_{24}F_{59}L_{26}$ (PF1, Permian), $Q_{29}F_{51}L_{20}$ (PF2, Middle Triassic), $Q_{31}F_{59}L_{10}$ (PF3, lower Upper Triassic), and $Q_{35}F_{42}L_{23}$ (PF4, Upper Triassic). The Pahau PF5 (Upper Jurassic to Lower Cretaceous) averages $Q_{27}F_{33}L_{40}$. The hexagons for each of these petrofacies and the sandstone clast populations are 95% confidence fields around the mean. Also shown are the five point-counted conglomerate clasts of MacKinnon (1980).

The Torlesse sandstone clasts are immature, moderately sorted, angular feldspathic arenites and have a restricted range of QFL compositions averaging $Q_{30}F_{49}L_{21}$ (Fig. 2B). The compositional change shown in the QFL diagram from one location to the next is mainly due to the slight increase in framework%Q from the Permian Te Moana Conglomerate to the Early Cretaceous Mount Saul Conglomerate. Framework lithic-fragment content follows a general reversed trend with a slight decrease in volcanic lithics but no significant change in L/Lv ratios. Framework feldspar content shows no significant change with time but the ratio of plagioclase to potassium feldspar decreases slightly. The following paragraphs summarise the salient points of each sandstone clast population.

The clast population from the Te Moana Conglomerate is the least mature with the lowest framework quartz content $Q_{26}F_{50}L_{24}$ and the highest P/F ratio compared with the other clast populations (Fig. 2B). Mean QFL values for the Te Moana and Lake Hill clasts show that there is no modal difference between the two clast populations. This is supported by P/F, Lv/L, and %M ratios, which are statistically indistinguishable. The Lake Hill clasts can be distinguished from the Te Moana clast population by a slightly higher framework%Q content, and compared with all other clast populations they have the lowest framework feldspar and %M content.

The sandstone clast population from the Ethelton Conglomerate is similar to that of the Mount Saul Conglomerate but can be distinguished by the lower framework%Q and %M mean content, higher lithic and P/F framework ratios, and a slightly higher Lv/L framework ratio. However, the Ethelton and Mount Saul differences are very slight and the 95% confidence fields of framework values and ratios overlap. The wide range in framework%Q in the Ethelton Conglomerate is mainly due to a couple of samples. One of these samples plots at the lithic-poor end of the measured range. QFL values show that the means of all the other clast populations plot within the Ethelton hexagon (Fig. 2B) and that the Ethelton clasts are compositionally similar to the other three sandstone clast populations.

The Aptian Mount Saul sandstone clast population can be distinguished from all the other populations by the highest framework%Q and %M content and the lowest lithic, P/F, and Lv/L ratio. Mean QFL parameters show that the Mount Saul clasts are statistically different from both Rakaia Terrane sandstone clast populations. On ternary compositional diagrams after Dickinson et al. (1983) and Ingersoll & Suczek (1979), the sandstones plot mainly in the dissected arc provenance field and the mixed magmatic arc field, respectively.

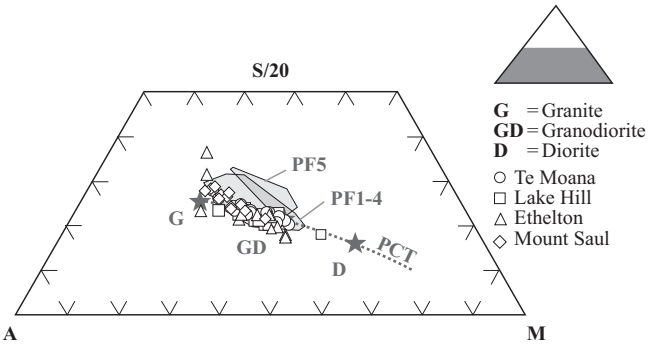

Fig. 4 SAM (Silica-Alkali-Mafic) plot (after Kroonenburg 1994) for sandstone clasts from the four conglomerate locations compared with Rakaia PF1–5 sandstones. The dotted line (PCT) is a primary igneous source composition line using the igneous averages from gabbro to granite of Le Maitre (1976). Diagram adapted from Roser & Korsch (1999). SAM: S = $SiO_2/20$; A = K_2O+Na_2O; M = $TiO_2+MgO+FeO_T$ (wt%).

Geochemistry

Roser et al. (1995) presented XRF analyses of Torlesse Terrane sandstones and argillites from the South Island and the southern part of the North Island. The authors analysed MacKinnon's (1980) petrofacies sandstones, and Roser et al. (1993) and Roser & Korsch (1999) used these data to confirm the geochemical validity of MacKinnon's (1980) South Island petrofacies scheme. The geochemical data from the four sandstone clast populations (Table 2) are compared with the geochemical data from the five Torlesse petrofacies of Roser et al. (1995). Matrix and diagenetic alteration in analysed sandstone clast samples is small (av. <9%; Table 1) and the chemistry of the samples therefore largely reflects the abundance of the detrital constituents.

Major elements

SiO_2 is relatively constant through the sandstone clast populations from 70.8 to 71.2 wt% but increases to 74.3 wt% in Mount Saul clasts with Al_2O_3 following a reverse trend (Table 2, Fig. 3A). This causes a slight increase in SiO_2/Al_2O_3 ratios for Te Moana, Lake Hill, and Ethelton clasts and a pronounced increase in the Mount Saul clast population. The steady increase of SiO_2/Al_2O_3 ratios from the Permian Te Moana to the Aptian Mount Saul sandstone clasts is consistent with the modal quartz content trends observed in clast petrography and reflects the maturity of detrital sediments, because this ratio increases as quartz is progressively concentrated at the expense of less resistant phases during weathering, transport, or recycling (Roser & Korsch 1988). At the same time there is a general decline of other components (TiO_2, Fe_2O_3 T, MgO, and CaO), which again is consistent with the increased quartz content of the sediments (Table 2). Roser & Korsch (1986) have demonstrated that K_2O/Na_2O ratio is a good indicator for sandstone type and tectonic setting and should also increase with sedimentary maturation as feldspars are converted to K-rich clays. The K_2O/Na_2O ratios increase steadily from the Permian Te Moana to the Aptian Mount Saul sandstone clast

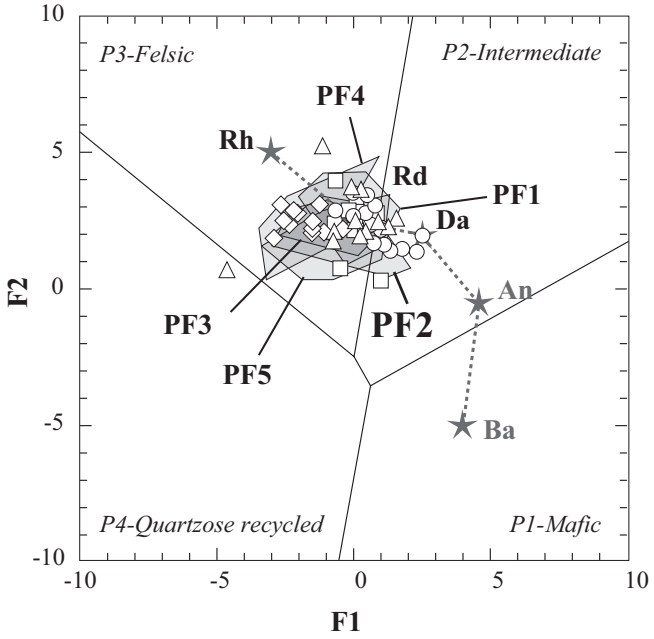

Fig. 5 Discriminant function plot (Roser & Korsch 1988) comparing the Rakaia and Pahau sandstone clast populations with Rakaia and Pahau Terrane sandstones. Fields PF1–5 and igneous averages Ba = basalt, An = andesite, Da = dacite, Rd = rhyodacite, and Rh = rhyolite are from Roser & Korsch (1988). F1 = $-1.773TiO_2 +0.607Al_2O_3 +0.76Fe_2O_3$ T $-1.5MgO +0.616CaO +0.509Na_2O -1.224K_2O -9.09$; F2 = $0.445TiO_2 +0.07Al_2O_3 -0.25Fe_2O_3$ T $-1.142MgO +0.438CaO +1.475Na_2O +1.426K_2O -6.861$.

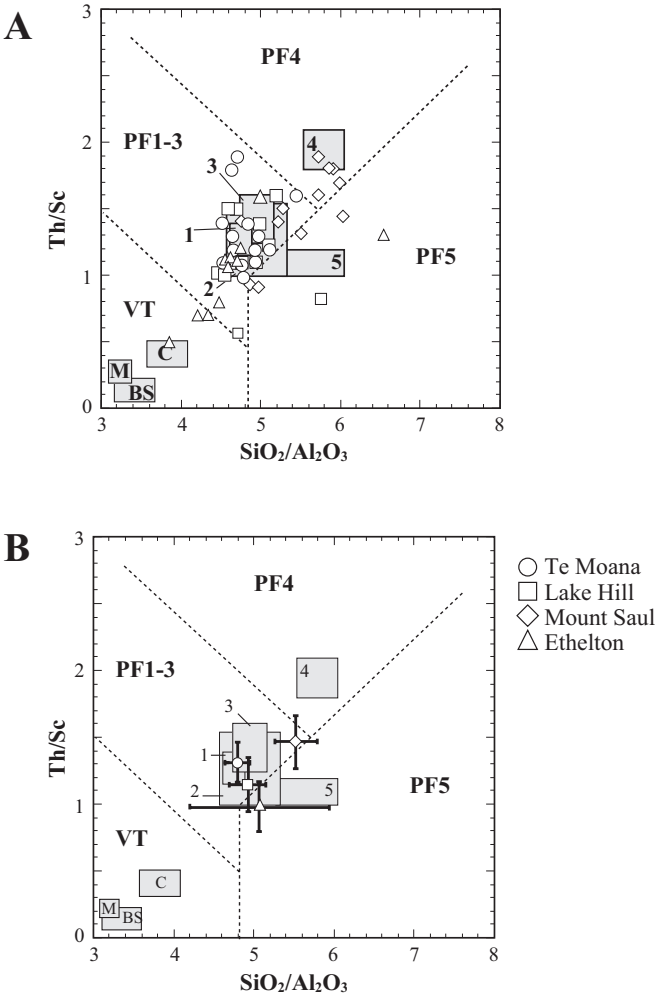

Fig. 6 **A**, Th/Sc-SiO_2/Al_2O_3 diagram for sandstone clasts from the four conglomerate locations compared with Torlesse PF1–5 sandstones. Petrofacies fields are from Roser & Korsch (1999). VT = volcanogenic terrane field, C = Caples Terrane, BS = Brook Street Terrane, M = Maitai Terrane. The boxes are 95% confidence interval fields and the numbers 1–5 are Torlesse petrofacies. **B**, Mean values and 95% confidence bars for the four sandstone clast populations.

populations (Fig. 2B), and the K_2O/Na_2O–SiO_2 relationship in all clast populations indicates an active continental margin.

On a Silica-Alkali-Mafic (SAM) diagram (Kroonenburg 1994), which partly mimics a QFL plot, clasts from Te Moana and Lake Hill lie generally along or just above the primary igneous compositional line (PCT), between granodiorite and granite (Fig. 4). Clasts from Ethelton lie slightly higher in the distribution than those from Te Moana and Lake Hill and are displaced slightly towards the SiO_2 apex. The wide extent of values for the Ethelton clast population reflects the petrographic range of this population.

A discriminant function plot has been proposed by Roser & Korsch (1988) to distinguish between sediments whose provenance is either primarily mafic, intermediate or felsic igneous, or a quartzose sediment. Most of the sandstone clasts plot within those fields close to the rhyodacite composition (Fig. 5).

A good measure of the degree of chemical weathering of the source rock can be obtained from the chemical index of alteration (CIA; Nesbitt & Young 1982), and values for the clast populations are shown in Table 2. The sandstone clast data from the four conglomerates lie within the established Torlesse compositional field of Roser & Korsch (1999).

Trace elements

Trace element parameters and discriminatory plots are a useful tool to further characterise the provenance and tectonic setting of clastic sediments (Bhatia & Crook 1986; McLennan et al. 1993). Although a large number of parameters can be used, the immobile trace elements (e.g., La, Th, Zr, Nb, Y, Sc, Co, and Ti) are particularly useful. Elements typically enriched in evolved felsic rocks or concentrated in more resistant minerals (e.g., Ce, La, Nd, Th, and Y) show no significant variation in average trace element concentration from the Permian Te Moana sandstone clasts (oldest conglomerate) to the Aptian Mount Saul sandstone populations (youngest conglomerate; Table 2). Overall trends show a slight increase from the Te Moana to the Lake Hill clast population and a general slight decline in concentrations from the Lake Hill to the Mount Saul clast population. Elements enriched in basic igneous rocks and associated with mafic minerals (Cr, Cu, Ni, Sc, V, and Zn) display a slight increase in concentrations over time.

Several trace element ratios have been used by Roser & Korsch (1999) to emphasise the patterns observed based on average element concentrations. The use of ratios formed between felsic- and mafic-linked elements maximises the contrast between the elements. The authors state that average ratios of Th/Sc, La/Sc, Ce/Sc, and La_N/Y_N should all increase in response to petrologic source evolution and/or maturation through recycling. Inverse ratios like V/La and Ti/Zr should

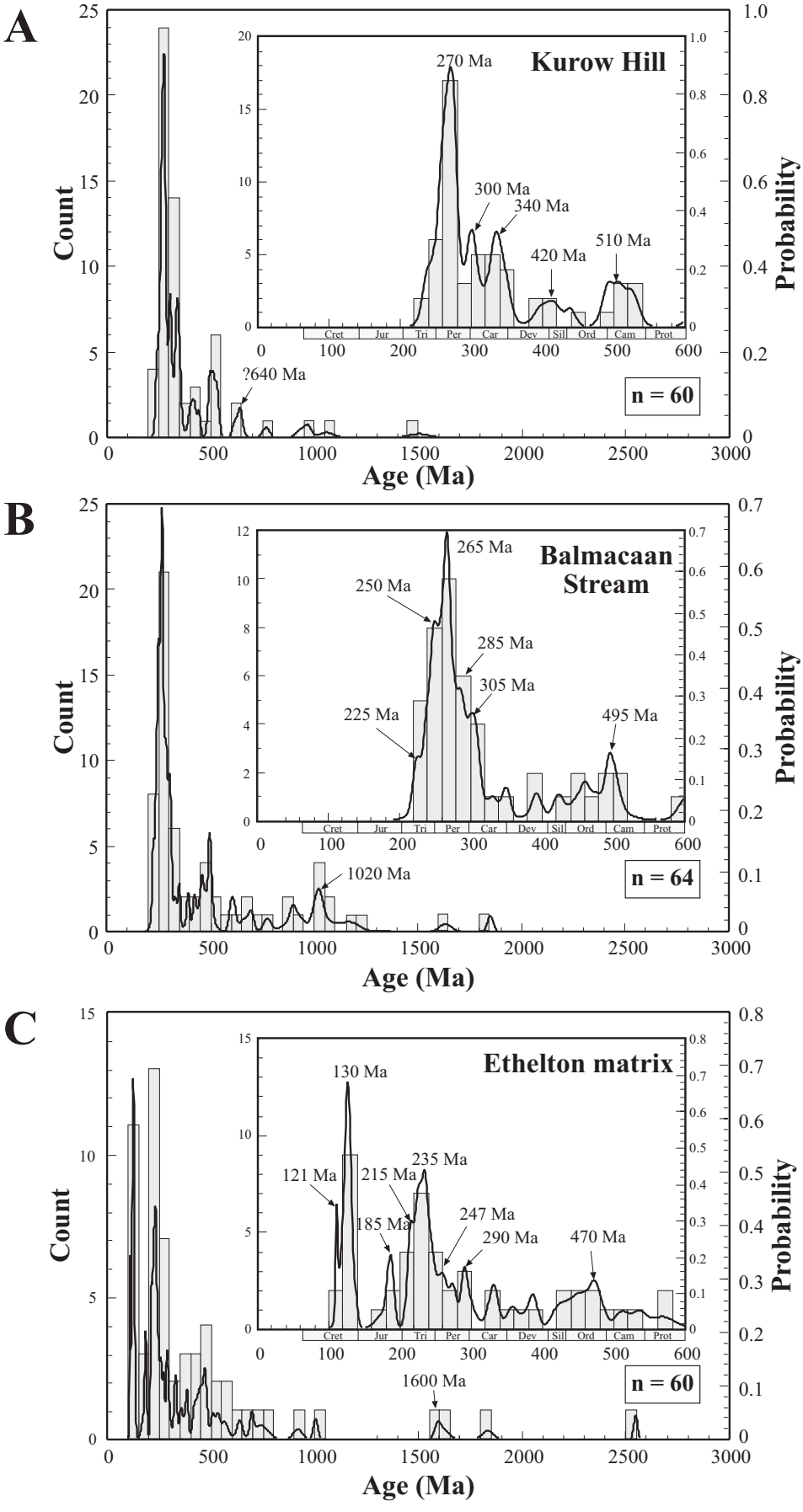

Fig. 7 **A**, U-Pb detrital zircon age histogram for the Kurow Hill sandstone. The age histogram is calculated at 50 m.y. intervals with counts shown on the left axis. The cumulative probability curve is calculated at 1 m.y. intervals (vertical scale on right axis). *Inset*: Histogram for the last 600 m.y. calculated at 20 m.y. intervals, with the cumulative probability curve calculated at 1 m.y. intervals. **B**, U-Pb detrital zircon age histogram for the Balmacaan Stream sandstone. **C**, U-Pb detrital zircon age histogram for the Ethelton : sandstone.

decrease with evolution, as mafic constituents decrease in abundance through petrologic evolution.

Ratios for Th/Sc and La/Sc show a steady decline in concentration from the Te Moana to the Ethelton clast population with a prominent increase of ratios between the clasts from Ethelton and Mount Saul (Fig. 3C,D). Ce/Sc increases slightly from the Te Moana to the Ethelton sandstone clasts with the biggest increase between the Ethelton and Mount Saul clasts. La_N/Y_N, which gives a measure of slope of rare earth (REE) patterns and has been normalised to the chondrite values of Taylor & McLennan (1985), decreases steadily from the Te Moana to the Ethelton clast population and ratios increase from the Ethelton to the Mount Saul clast population (Fig. 3F). Inverse ratios for V/La and Ti/Zr show a positive correlation with decreasing depositional age, with a steady increase from the Te Moana to the Ethelton clast population and a distinct decline in concentration between the sandstone population of Ethelton and Mount Saul. This pattern is consistent with the pattern displayed by the ratios for Th/Sc, La/Sc, and La_N/Y_N.

When plotted on a SiO_2/Al_2O_3–Th/Sc diagram (Fig. 6), the sandstone clasts from the two Rakaia conglomerates show a narrow range of SiO_2/Al_2O_3 ratios (4.5–5.8) and Th/Sc ratios (0.6–1.9). Values are confined to the field of PF1–3, with only one clast plotting in the field of PF5. Petrographically, this clast has the highest quartz content, one of the highest mafic contents, and one of the lowest total feldspar contents. The trace element ratios of almost all the Rakaia sandstone clasts are geochemically indistinguishable from PF1–3.

Pahau Terrane clasts display a slightly wider range of SiO_2/Al_2O_3 ratios (3.8–6.5) but Th/Sc ratios (0.5–1.9) are similar to the ratios displayed by the Rakaia sandstone clasts. However, clasts from the Mount Saul Conglomerate plot within all the Torlesse petrofacies fields and are the only clasts that extend into PF4. Clasts from Ethelton generally plot within the PF1–3 field but extend into the volcanogenic field. In contrast to the maturation trend observed in SiO_2/Al_2O_3–Th/Sc ratios from PF1–4 Torlesse sandstones as noted by Roser & Korsch, mean values for the Permian Te Moana to the Barremian Ethelton sandstone clast population display an inverse trend with a pronounced increase in the Mount Saul clast mean values (Fig. 6B). This trend is consistent with trends observed in other trace element concentration ratios of the sandstone clasts.

Detrital U-Pb zircon ages

U-Pb ages for two Rakaia Terrane sandstones (Kurow, Balmacaan localities; Fig. 1) and for a matrix sample of the Ethelton Conglomerate were obtained and are listed in Table 3. Data for the individual detrital samples are presented in Fig. 7 as age histograms with a calculated interval of 20 m.y. Sample age distributions are summaries in terms of major age components (usually 5%), but some minor groups are also identified when a peak is noted. The groups identified in each dataset are defined by natural breaks in the data. The age histograms are overlain by cumulative probability curves to further highlight the principal age components.

Kurow

Of the 60 analysed zircon grains, 70% are represented by the age group with ages between 349 and 237 Ma (Fig. 7A). The group is a complex cluster of three distinct peaks at c. 340, 300, and 270 Ma with the main peak making up 28% of the data. The group between 260 and 240 Ma (10%) has a peak at c. 255 Ma. A minor Middle Devonian–Silurian group (6%) at 420–380 Ma has a peak at c. 420 Ma and an Ordovician to Early Cambrian group (540–480 Ma) makes up 12% of the data with a broad peak at c. 510 Ma. The remaining six analyses range from 1499 to 630 Ma and make up 10% of the data with a minor peak (6%) at 640 Ma and insignificant peaks (3%) at 966, 1050, and 1500 Ma. Cores of the two youngest zircons from this sandstone returned Middle Triassic (Anisian) 239 ± 6 Ma and 238 ± 8 Ma ages. The weighted mean age of the four youngest zircons is 242.5 ± 3.6 Ma (1 σ; MSWD = 0.62). This youngest principal age component is in disagreement with the Permian stratigraphic age based on fossils. An Early Triassic (Spathian) depositional age is indicated for the Kurow Hill area.

Balmacaan Stream

A total of 64 zircons were analysed from this sandstone sample (Fig. 7B). The major Late Triassic–Carboniferous (Namurian) group comprises 51% of the whole data, with the main peak (16%) between 280 and 260 Ma at c. 265 Ma, and two minor younger peaks at c. 250 Ma (13%) and 230 Ma (8%). The group between 320 and 280 Ma make up 15% of all the analyses and there are two possible peaks at 285 Ma (9%) and 305 Ma (6%). There are insignificant peaks (<5%) between the Carboniferous and the Ordovician (480–320 Ma) and one minor group between 520 and 480 Ma (6%) with a peak at 495 Ma. The remaining analyses (28%) extend to 1848 Ma with minor groups at 929–870 Ma (5%) and 1085–1004 Ma (9%) with a peak at c. 1020 Ma. The three youngest zircons from this sandstone returned a weighted mean age of 225.1 ± 4.1 Ma (1 σ; MSWD = 0.35). This Late Triassic (Carnian) age is proposed as the maximum stratigraphic age for the Balmacaan Stream conglomerate.

Ethelton

A total of 60 zircons were analysed from this sample (Fig. 7C). Two distinct main groups are recognised, one in the Cretaceous with an age range of 135–112 Ma and a second extending from the Carboniferous to the Late Triassic (300–214 Ma). The main peak of the Cretaceous group is within the age range of 140–120 Ma (15%) at c. 130 Ma. The youngest zircon (111.7 ± 1.4 Ma) has a very high U concentration (2012 ppm) and this age is regarded as suspicious. The weighted mean age of the three youngest zircons is 121.0 ± 3.1 Ma (1 σ; MSWD = 0.03), indicating a Barremian maximum stratigraphic age. The second group (33%) consists of a mixture of peaks with the main peak at c. 230 Ma (260–200 Ma; 25%), a minor peak at c. 290 Ma (300–280 Ma; 5%), and two possible minor peaks at c. 215 Ma (220–200 Ma; 7%), and 247 Ma (260–240 Ma; 7%). There is a minor Early Jurassic group (187–176 Ma; 5%) with a peak at c. 185 Ma. A broad Silurian–Cambrian group (540–420 Ma; 15%) has a peak at c. 470 Ma. There is a subdued Devonian peak at c. 385 Ma (400–360 Ma). The remaining 10 analyses make up 17% of the data and extend into the Archean (2548 Ma) with a possible peak at 1627–1594 Ma.

Table 3 U/Pb analyses of detrital zircons from Torlesse sediments at Kurow, Balmacaan Stream, and Ethelton.

Grain	U (ppm)	Th (ppm)	Th/U	$^{207}Pb/^{206}Pb$	$^{238}U/^{206}Pb$	Age (Ma)
Kurow Hill						
K-29	119	74	0.62	0.0535 ± 0.0169	26.65 ± 0.86	237.5 ± 7.5
K-30	220	123	0.56	0.0512 ± 0.0128	26.49 ± 0.68	238.9 ± 6
K-16	523	366	0.7	0.0505 ± 0.008	25.54 ± 0.84	247.6 ± 8
K-45	226	270	1.19	0.0253 ± 0.0173	25.43 ± 0.79	248.6 ± 7.6
K-43	417	214	0.51	0.041 ± 0.0142	24.55 ± 0.56	257.4 ± 5.7
K-37	118	101	0.85	0.0468 ± 0.0222	24.5 ± 1.08	257.9 ± 11.2
K-39	1694	956	0.56	0.0536 ± 0.0024	24.4 ± 0.37	259 ± 3.9
K-55	85	82	0.96	–0.0338 ± 0.0608	24.32 ± 2.13	259.7 ± 22.3
K-31	458	259	0.57	0.0619 ± 0.0114	24.12 ± 0.52	262 ± 5.5
K-11	209	137	0.66	0.0341 ± 0.0108	23.76 ± 0.65	265.8 ± 7.2
K-12	293	214	0.73	0.0461 ± 0.0092	23.7 ± 0.45	266.4 ± 4.9
K-28	995	765	0.77	0.0484 ± 0.0029	23.56 ± 0.61	267.6 ± 6.8
K-32	107	36	0.34	0.0579 ± 0.0268	23.59 ± 1.01	267.7 ± 11.3
K-24	253	148	0.58	0.0532 ± 0.0214	23.44 ± 0.98	269.4 ± 11
K-17	499	359	0.72	0.0474 ± 0.0073	23.25 ± 0.58	271.4 ± 6.6
K-14	515	290	0.56	0.0481 ± 0.0034	23.17 ± 0.37	272.2 ± 4.2
K-3	426	315	0.74	0.0478 ± 0.0072	23.14 ± 0.71	272.6 ± 8.2
K-52	389	225	0.58	0.0407 ± 0.0077	23.07 ± 0.49	273.6 ± 5.7
K-49	1902	2163	1.14	0.051 ± 0.0015	23.01 ± 0.41	274.1 ± 4.8
K-10	439	252	0.57	0.0558 ± 0.0135	22.91 ± 0.63	275.5 ± 7.5
K-33	272	161	0.59	0.0567 ± 0.0073	22.89 ± 0.52	275.8 ± 6.1
K-26	382	202	0.53	0.0539 ± 0.0066	22.82 ± 0.47	276.5 ± 5.6
K-20	493	180	0.37	0.0534 ± 0.0039	22.76 ± 0.32	277.3 ± 3.8
K-4	94	59	0.63	0.0573 ± 0.0146	22.56 ± 0.81	279.7 ± 9.8
K-7	177	71	0.4	0.0484 ± 0.0091	22.53 ± 0.79	280 ± 9.7
K-8	154	87	0.56	0.0467 ± 0.0137	22.35 ± 0.77	282.2 ± 9.5
K-36	141	125	0.89	0.0595 ± 0.0184	21.56 ± 0.62	292.4 ± 8.2
K-5	860	304	0.35	0.0496 ± 0.0026	21.06 ± 0.41	298.9 ± 5.7
K-13	2145	415	0.19	0.0531 ± 0.0014	20.84 ± 0.33	302.4 ± 4.7
K-60	236	223	0.95	0.0524 ± 0.0127	20.6 ± 0.49	305.6 ± 7.1
K-2	144	59	0.41	0.0512 ± 0.0126	20.51 ± 0.51	306.9 ± 7.5
K-41	201	82	0.41	0.0642 ± 0.0111	20.45 ± 0.59	308 ± 8.7
K-21	97	70	0.72	0.0334 ± 0.0325	20.24 ± 0.96	310.9 ± 14.4
K-50	254	138	0.54	0.0475 ± 0.0109	19.33 ± 0.46	325.2 ± 7.5
K-57	158	98	0.62	0.0407 ± 0.0197	19.09 ± 0.61	329.2 ± 10.2
K-54	441	116	0.26	0.0552 ± 0.004	18.83 ± 0.33	333.6 ± 5.6
K-58	623	471	0.76	0.0531 ± 0.0039	18.74 ± 0.41	335.1 ± 7.2
K-9	333	219	0.66	0.052 ± 0.0042	18.73 ± 0.35	335.3 ± 6.1
K-53	393	230	0.59	0.0499 ± 0.0045	18.34 ± 0.32	342.1 ± 5.8
K-1	314	166	0.53	0.0494 ± 0.0056	18.04 ± 0.39	347.6 ± 7.4
K-44	246	73	0.3	0.0549 ± 0.0109	17.98 ± 0.42	349 ± 7.9
K-59	445	210	0.47	0.0513 ± 0.0039	17.93 ± 0.51	349.6 ± 9.7
K-6	36	14	0.39	–0.003 ± 0.0623	16.13 ± 1.34	387.7 ± 31.4
K-34	152	55	0.37	0.0534 ± 0.0114	15.67 ± 0.36	398.9 ± 8.9
K-38	108	101	0.93	0.0695 ± 0.0131	15.02 ± 0.49	415.9 ± 13.3
K-42	564	224	0.4	0.0556 ± 0.0024	14.95 ± 0.32	417.6 ± 8.7
K-18	636	403	0.63	0.0553 ± 0.0026	14.11 ± 0.24	441.3 ± 7.1
K-40	199	80	0.4	0.0584 ± 0.0054	12.72 ± 0.22	488 ± 8.2
K-23	160	105	0.66	0.0658 ± 0.0046	12.33 ± 0.36	505.3 ± 14.2
K-51	897	254	0.28	0.0581 ± 0.003	12.23 ± 0.16	506.8 ± 6.5
K-56	188	111	0.59	0.0442 ± 0.0104	12.22 ± 0.29	507.3 ± 11.5
K-19	747	117	0.16	0.06 ± 0.0014	11.96 ± 0.29	522.2 ± 11.7
K-25	231	85	0.37	0.0575 ± 0.0039	11.73 ± 0.28	527.1 ± 11.9
K-47	689	245	0.36	0.0587 ± 0.0014	11.72 ± 0.21	528.5 ± 8.8
K-48	640	123	0.19	0.0641 ± 0.0014	9.67 ± 0.16	638.9 ± 9.7
K-15	326	294	0.9	0.0598 ± 0.0028	9.55 ± 0.25	640.8 ± 15.6
K-22	720	89	0.12	0.0689 ± 0.0016	8.14 ± 0.2	764.4 ± 16.3
K-35	205	223	1.09	0.0774 ± 0.0035	6.22 ± 0.11	966.5 ± 15.5
K-27	1070	208	0.19	0.0745 ± 0.0013	7 ± 0.13	1053.7 ± 34.1
K-46	99	52	0.52	0.0947 ± 0.005	3.84 ± 0.15	1499.1 ± 47

Table 3 *(continued)*

Grain	U (ppm)	Th (ppm)	Th/U	$^{207}Pb/^{206}Pb$	$^{238}U/^{206}Pb$	Age (Ma)
Balmacaan Stream						
B-49	360	338	0.94	0.0811 ± 0.0064	28.42 ± 0.63	222.9 ± 4.8
B-16	96	181	1.87	0.0477 ± 0.0498	27.52 ± 2.1	230.1 ± 17.3
B-31	128	127	0.99	0.0663 ± 0.0223	27.43 ± 1.07	230.9 ± 8.9
B-59	113	97	0.86	0.0549 ± 0.0174	26.75 ± 0.97	236.6 ± 8.4
B-4	289	224	0.78	0.0568 ± 0.0031	26.66 ± 0.45	237.7 ± 3.9
B-30	667	365	0.55	0.0523 ± 0.0053	25.77 ± 0.42	245.5 ± 4
B-29	163	130	0.8	0.0531 ± 0.0235	25.69 ± 0.87	246.2 ± 8.2
B-28	1273	777	0.61	0.0532 ± 0.0047	25.53 ± 0.41	247.7 ± 3.9
B-47	151	147	0.97	0.0197 ± 0.0243	25.25 ± 1	250.4 ± 9.7
B-64	185	136	0.74	0.0445 ± 0.0186	25.23 ± 0.7	250.5 ± 6.8
B-61	392	301	0.77	0.051 ± 0.0061	25.02 ± 0.52	252.6 ± 5.2
B-42	239	172	0.72	0.0499 ± 0.0127	24.69 ± 0.57	256 ± 5.8
B-39	276	147	0.53	0.0495 ± 0.0141	24.47 ± 0.54	258.2 ± 5.6
B-58	283	98	0.35	0.05 ± 0.0107	24.25 ± 0.55	260.5 ± 5.8
B-50	225	220	0.98	0.0767 ± 0.0043	24.19 ± 0.49	261.2 ± 5.2
B-21	262	207	0.79	0.0618 ± 0.0168	23.97 ± 0.75	263.6 ± 8.1
B-45	467	210	0.45	0.0486 ± 0.0035	23.79 ± 0.33	265.4 ± 3.7
B-12	251	262	1.04	0.0412 ± 0.012	23.69 ± 0.54	266.6 ± 5.9
B-27	407	190	0.47	0.0494 ± 0.0067	23.66 ± 0.38	266.8 ± 4.2
B-53	471	289	0.61	0.0522 ± 0.0042	23.64 ± 0.47	267.1 ± 5.2
B-51	383	335	0.87	0.0508 ± 0.004	23.5 ± 0.36	268.6 ± 4.1
B-36	251	278	1.11	0.0529 ± 0.0115	23.24 ± 0.46	271.6 ± 5.2
B-54	316	122	0.39	0.0508 ± 0.0059	22.9 ± 0.41	275.5 ± 4.9
B-24	241	118	0.49	0.0382 ± 0.008	22.42 ± 0.42	281.3 ± 5.1
B-62	228	101	0.44	0.0532 ± 0.016	22.37 ± 0.62	281.9 ± 7.6
B-34	229	205	0.89	0.0502 ± 0.021	22.03 ± 0.68	286.2 ± 8.7
B-35	272	215	0.79	0.0532 ± 0.0079	22 ± 0.51	286.6 ± 6.5
B-15	402	231	0.57	0.0555 ± 0.0071	21.91 ± 0.37	287.7 ± 4.7
B-32	293	329	1.12	0.0449 ± 0.0055	21.19 ± 0.36	297.3 ± 4.9
B-60	326	236	0.72	0.0494 ± 0.0069	20.72 ± 0.6	303.8 ± 8.7
B-56	356	383	1.07	0.0571 ± 0.0069	20.72 ± 0.41	303.9 ± 5.8
B-19	207	155	0.75	0.0569 ± 0.0249	20.65 ± 0.69	304.9 ± 9.9
B-23	281	159	0.57	0.0567 ± 0.0087	20.47 ± 0.39	307.6 ± 5.7
B-20	238	194	0.81	0.065 ± 0.0103	19.05 ± 0.46	330 ± 7.7
B-46	543	245	0.45	0.0548 ± 0.0031	17.98 ± 0.3	349 ± 5.6
B-8	203	144	0.71	0.3769 ± 0.1471	16.29 ± 2	384 ± 45.8
B-52	147	85	0.58	0.0577 ± 0.0061	15.97 ± 0.29	391.8 ± 7
B-1	422	169	0.4	0.0559 ± 0.0017	14.78 ± 0.26	422.4 ± 7.2
B-5	146	101	0.69	0.0759 ± 0.0113	13.97 ± 0.3	446.3 ± 9.3
B-26	998	601	0.6	0.0562 ± 0.0026	13.54 ± 0.19	459.4 ± 6.2
B-13	345	94	0.27	0.0501 ± 0.0077	13.1 ± 0.22	474 ± 7.8
B-44	406	153	0.38	0.0593 ± 0.0026	12.57 ± 0.15	493.7 ± 5.7
B-33	136	46	0.34	0.0492 ± 0.0135	12.46 ± 0.27	497.7 ± 10.3
B-18	331	130	0.39	0.0607 ± 0.0058	12.4 ± 0.22	500 ± 8.5
B-57	826	119	0.14	0.0584 ± 0.0029	12.39 ± 0.6	502.2 ± 22.8
B-38	633	77	0.12	0.0647 ± 0.0024	10.34 ± 0.21	598.5 ± 11.2
B-43	165	81	0.49	0.0575 ± 0.008	10.02 ± 0.2	613.2 ± 11.7
B-37	264	141	0.53	0.0747 ± 0.0096	9.29 ± 0.28	660.9 ± 19.1
B-22	530	333	0.63	0.0661 ± 0.0028	8.8 ± 0.17	696.1 ± 12.9
B-7	311	163	0.53	0.2867 ± 0.601	8.79 ± 4.84	726.9 ± 371.2
B-25	359	30	0.08	0.0731 ± 0.0042	7.91 ± 0.21	773.9 ± 18.9
B-2	58	19	0.32	0.0801 ± 0.0061	7.02 ± 0.27	871 ± 30.7
B-6	172	46	0.27	0.0715 ± 0.0022	6.73 ± 0.12	896.6 ± 14.2
B-41	248	74	0.3	0.0707 ± 0.0044	6.45 ± 0.16	930 ± 21.2
B-63	127	76	0.6	0.0732 ± 0.0046	5.93 ± 0.12	1004.4 ± 18.8
B-17	273	74	0.27	0.0697 ± 0.0033	5.79 ± 0.11	1023.5 ± 17.1
B-11	353	61	0.17	0.0752 ± 0.0025	5.8 ± 0.13	1029.4 ± 20.6
B-55	908	123	0.14	0.0738 ± 0.0022	7.33 ± 0.09	1034.7 ± 60.4
B-10	335	91	0.27	0.124 ± 0.0706	5.53 ± 0.43	1074.1 ± 76.8
B-40	218	72	0.33	0.0756 ± 0.0031	8.28 ± 0.2	1085.5 ± 84.6
B-3	136	51	0.38	0.0947 ± 0.0194	4.99 ± 0.18	1181.2 ± 39.1
B-9	196	53	0.27	0.196 ± 0.3012	4.92 ± 1.47	1214.8 ± 331
B-48	574	239	0.42	0.1005 ± 0.0016	5.43 ± 0.09	1632.5 ± 30.2
B-14	584	313	0.54	0.113 ± 0.0009	3.56 ± 0.04	1848.4 ± 14.9

(continued)

Table 3 *(continued)*

Grain	U (ppm)	Th (ppm)	Th/U	$^{207}Pb/^{206}Pb$	$^{238}U/^{206}Pb$	Age (Ma)
Ethelton						
E-18	2012	1615	0.8	0.0475 ± 0.0014	57.18 ± 0.75	111.8 ± 1.4
E-13	738	284	0.38	0.0509 ± 0.0098	53.36 ± 2.97	119.7 ± 6.6
E-41	318	157	0.49	0.0429 ± 0.0165	52.73 ± 2.17	121.1 ± 4.9
E-27	83	81	0.97	0.0133 ± 0.0273	52.5 ± 2.19	121.6 ± 5
E-28	1464	1359	0.93	0.0481 ± 0.0018	51.13 ± 1.31	124.8 ± 3.2
E-26	40	25	0.64	0.0472 ± 0.0383	51.12 ± 3.35	124.9 ± 8.1
E-57	955	414	0.43	0.0532 ± 0.0019	50.63 ± 0.88	126.2 ± 2.2
E-21	358	274	0.77	0.0549 ± 0.0236	49.76 ± 1.85	128.3 ± 4.7
E-47	436	242	0.55	0.057 ± 0.0024	49.2 ± 1.3	129.7 ± 3.4
E-55	598	264	0.44	0.0849 ± 0.0068	48.97 ± 0.85	130.3 ± 2.3
E-44	413	276	0.67	0.0519 ± 0.0047	47.17 ± 1.42	135.3 ± 4
E-14	68	61	0.91	-0.0159 ± 0.0305	36.08 ± 2.08	176.2 ± 10
E-9	362	311	0.86	0.0496 ± 0.0064	34.13 ± 0.8	186.2 ± 4.3
E-22	269	188	0.7	0.0521 ± 0.0083	33.86 ± 0.81	187.6 ± 4.4
E-60	462	234	0.51	0.0686 ± 0.0032	29.69 ± 0.49	213.5 ± 3.5
E-51	1341	585	0.44	0.0528 ± 0.0013	29.75 ± 0.69	213.9 ± 4.9
E-32	251	217	0.86	0.0505 ± 0.0094	28.95 ± 0.89	218.9 ± 6.6
E-42	326	220	0.67	0.054 ± 0.0033	28.87 ± 0.57	219.6 ± 4.3
E-48	524	326	0.62	0.0521 ± 0.0026	28.15 ± 0.5	225.1 ± 3.9
E-19	506	229	0.45	0.0504 ± 0.0028	27.97 ± 0.47	226.5 ± 3.7
E-24	528	479	0.91	0.0498 ± 0.0029	27.59 ± 0.61	229.5 ± 5
E-12	878	421	0.48	0.0522 ± 0.0029	27.21 ± 0.46	232.7 ± 3.8
E-53	740	556	0.75	0.0583 ± 0.0014	26.94 ± 0.39	235 ± 3.4
E-10	336	149	0.44	0.0577 ± 0.0021	26.7 ± 0.67	237.1 ± 5.9
E-11	422	335	0.79	0.05 ± 0.0034	26.53 ± 0.86	238.4 ± 7.6
E-43	208	86	0.41	0.0542 ± 0.0059	26.2 ± 0.59	241.5 ± 5.3
E-45	174	141	0.81	0.0496 ± 0.0053	25.89 ± 0.58	244.3 ± 5.4
E-17	254	138	0.54	0.0644 ± 0.0086	24.62 ± 0.84	257.1 ± 8.6
E-38	129	80	0.62	0.055 ± 0.0063	24.36 ± 0.68	259.5 ± 7.1
E-2	522	265	0.51	0.051 ± 0.0052	24.2 ± 0.75	261 ± 7.9
E-25	2500	5178	2.07	0.0486 ± 0.0059	22.98 ± 0.36	274.6 ± 4.2
E-8	2110	2709	1.28	0.0539 ± 0.0012	21.81 ± 0.34	289.5 ± 4.4
E-58	442	212	0.48	0.055 ± 0.0022	21.57 ± 0.53	292.9 ± 7
E-5	45	29	0.64	0.0647 ± 0.0053	21.17 ± 0.82	299.3 ± 11.2
E-50	300	118	0.39	0.0546 ± 0.0017	19.08 ± 0.44	330 ± 7.4
E-29	611	247	0.4	0.0584 ± 0.0031	18.98 ± 0.35	331.5 ± 6
E-1	103	60	0.58	0.0569 ± 0.0086	17.59 ± 0.37	356.4 ± 7.2
E-4	164	74	0.45	0.0556 ± 0.0029	16.61 ± 0.46	377.2 ± 10.1
E-59	550	157	0.28	0.0647 ± 0.0016	16.16 ± 0.25	387.1 ± 5.9
E-20	144	50	0.35	0.0443 ± 0.0058	14.85 ± 0.33	420.2 ± 9
E-6	113	40	0.35	0.0604 ± 0.0072	14.34 ± 0.41	434.8 ± 12
E-36	341	270	0.79	0.0557 ± 0.0033	14.05 ± 0.34	443.3 ± 10.4
E-3	314	155	0.49	0.0605 ± 0.0025	13.66 ± 0.3	457.1 ± 9.6
E-37	207	37	0.18	0.0565 ± 0.0054	13.44 ± 0.36	462.8 ± 11.8
E-31	2355	589	0.25	0.059 ± 0.0012	13.24 ± 0.18	471.1 ± 6.2
E-23	458	193	0.42	0.0661 ± 0.0029	12.93 ± 0.2	480.4 ± 7.3
E-35	193	78	0.41	0.0602 ± 0.0032	12.16 ± 0.24	510 ± 9.5
E-46	346	176	0.51	0.0596 ± 0.0022	11.58 ± 0.22	534.6 ± 9.8
E-54	497	51	0.1	0.0644 ± 0.0015	10.87 ± 0.3	567.1 ± 14.9
E-15	2048	519	0.25	0.0591 ± 0.0018	23.92 ± 0.76	570.2 ± 69.2
E-39	861	87	0.1	0.0642 ± 0.0012	9.76 ± 0.21	640.6 ± 12.3
E-7	903	67	0.07	0.063 ± 0.0009	8.75 ± 0.13	698.2 ± 9.4
E-56	1291	249	0.19	0.0636 ± 0.0007	11.36 ± 0.18	729.1 ± 22.9
E-40	547	103	0.19	0.0679 ± 0.0022	8.13 ± 0.32	763.8 ± 25.6
E-33	173	59	0.34	0.0733 ± 0.0025	6.6 ± 0.17	920.2 ± 21.2
E-49	969	290	0.3	0.0742 ± 0.001	5.97 ± 0.07	1005.4 ± 10.5
E-34	1679	923	0.55	0.0984 ± 0.0008	4.03 ± 0.08	1594.1 ± 15.2
E-52	263	145	0.55	0.1044 ± 0.0024	3.57 ± 0.07	1627.3 ± 23.8
E-30	287	197	0.69	0.1122 ± 0.0015	3.92 ± 0.07	1834.5 ± 24.5
E-16	511	320	0.63	0.1691 ± 0.0009	2.7 ± 0.05	2548.3 ± 8.9

DISCUSSION

Comparison of sandstone clasts and Torlesse sandstones

Compared with Torlesse sandstones (Fig. 2B), the clasts from Te Moana show strong affinities with PF1 (Permian) and only minor overlap with PF2 (Middle Triassic). The P/F ratio compares well with the PF1 value. However, Lv/L ratios are higher, and %M are slightly lower than PF1 values and are more compatible with PF2–4. QFL values for the Lake Hill clasts show an equal overlap with PF1 and PF2, and Lv/L and P/F ratio values fall within the range of the PF2–4 values. Compared with the Torlesse sandstone petrofacies, the Ethelton sandstone clast population shows strong affinities with PF2. The other parameters, P/F and Lv/L ratios, compare well with PF2–4. The Mount Saul clasts plot between PF3 (Middle Triassic) and PF4 (Late Triassic). The Lv/L ratio falls within the range of PF2–4 but P/F is slightly lower than all PF values.

Based on the distinct QFL shift in PF4–5 (Fig. 2B), decrease in Lv/L, increase in sedimentary lithics of Torlesse derivation, and the presence of detrital pumpellyite in PF5, MacKinnon (1983) proposed that the compositions of these younger petrofacies were influenced by the reworking of indurated and metamorphosed sediments from PF1–3. The gradual and progressive change through time of Torlesse sandstone compositions relate to the evolution of the source and gradual unroofing of a continental margin volcano/plutonic arc that was still active during the deposition of PF1–3. Uplifted and metamorphosed older Rakaia rocks became the dominant supplier to the trench to form the younger Pahau Terrane. Petrographic observations made in the sandstone clast populations lend support to MacKinnon's idea. Petrography of the four sandstone clast populations strongly suggests that:

(1) autocannibalistic reworking of PF1 sandstone is a major source for the Permian Te Moana Conglomerate sandstone clasts;
(2) sandstone clasts in the Lake Hill Conglomerate are derived by autocannibalistic recycling of PF1–2 sandstones;
(3) older rocks from PF2 and sandstones in composition between PF3 and PF4, are the main sandstone clast supplier to the younger Pahau conglomerates.

Geochemically, the observed trend in the SAM plot (Fig. 5) mirrors the trend observed in the QFL diagram. The Rakaia PF1–4 petrofacies data occupy a relatively small field and are geochemically almost indistinguishable with most of the clasts plotting within this field, whereas only a few clasts plot within the field of the Pahau PF5. A similar trend is observed in the discriminant function plot (Fig. 5). However, PF4 shows a slightly different distribution from PF1–3, in plotting at the most felsic end and also extending down towards the PF3/4 boundary (consistent with maturation through cannibalistic recycling). Although there is some overlap with PF1–3, virtually all PF5 samples of MacKinnon (1980) plot below the line of igneous averages and also extend down towards the PF3/4 boundary but at a lower F2 than PF4, reflecting the minor mafic volcanogenic input inferred by Roser & Korsch (1999) and apparent in MacKinnon's modes. Almost none of the sandstone clast samples plot in the area in which only Pahau sandstones fall, giving major element support to the petrographic identification of the clasts as Rakaia.

Chemical index of alteration values from the four clast populations show little variation (53.1–55.2), with a mean of 54 that is comparable to those of feldspar (CIA = 50) and unweathered felsic plutonic and volcanic rocks (45–55) (Fedo et al. 1995). Thin-section observations are consistent and show virtually unweathered and angular feldspar. The CIA ratios indicate that the clast source has undergone very little chemical weathering before deposition, despite the indication that the source was a dissected arc, suggesting that uplift had to be fairly rapid, so fresh material was continuously exposed and eroded.

Although there are some anomalies, trace element concentrations for the sandstone clasts generally are similar to PF1–4 values published by Roser & Korsch (1999, table 4.3), who ascribed the observed trace element variations to an initial source variability and the effect of partial recycling of earlier petrofacies. Roser & Korsch showed that small changes in elemental ratios in Rakaia Terrane PF1–3 parallel petrographic QFL trends, reflecting an initial source control. Local recycling into PF4, coupled with a small influx of volcanic detritus, lead to contrasts in provenance-linked indices (e.g., SiO_2/Al_2O_3, K_2O/Na_2O, Th/Sc, La/Sc, Ce/Sc).

In summary, the sandstone clasts from the four conglomerates and PF1–5 sandstones are derived from a relatively unweathered source with an average composition similar to that of rhyodacite. Sandstone clast major and trace element chemical data largely support petrographic observations derived from thin-section analysis. Overall, the slight increase in modal quartz content from the Permian Te Moana to the Early Cretaceous sandstone clast populations is consistent with the maturation trend displayed by the major element ratios SiO_2/Al_2O_3 and K_2O/Na_2O. At the same time, elements associated with mafic minerals (e.g., TiO_2, Fe_2O_3, MgO, and CaO) display inverse trends. However, the maturation trend is not reflected in trace element concentrations, which vary only slightly between all the sandstone clast populations.

Recycling of the Rakaia Terrane

The abrupt change in elemental abundance and indices between PF3 and PF4 is mirrored by the chemistry of the sandstone clasts from Ethelton and Mount Saul (Fig. 3, 6). The changes in SiO_2/Al_2O_3, K_2O/Na_2O, trace element ratios, and elemental abundance between PF3 and PF4 are generally consistent with sedimentological maturation produced by the onset of recycling, as proposed by MacKinnon (1983) and Roser & Korsch (1999). Mean trace element ratios of the four sandstone clast populations show that all sandstone clasts have strong affinities with PF1–3 sandstones. There is a negative correlation between Th/Sc, La/Sc, and La_N/Y_N ratios with decreasing depositional age from the Te Moana to the Ethelton clasts. This negative trend is in agreement with the positive relationship between depositional age and V/La and Ti/Zr ratios. Thus, the trend observed in the Te Moana/Lake Hill/Ethelton trace element ratios is toward slightly more primitive material as the depositional ages decrease. This trend contradicts the slight maturation trend for PF1–3 trace element concentration ratios reported by Roser & Korsch (1999) and most likely reflects the exhumation of older Rakaia Terrane rocks.

The first regional metamorphic event recognised in the Rakaia Terrane is attributed to the Caples/Torlesse Terrane collision (e.g., Mortimer 1993, and references therein). The similarities of petrographic data, chemical compositions, and ratios between sandstone clasts from the Rakaia

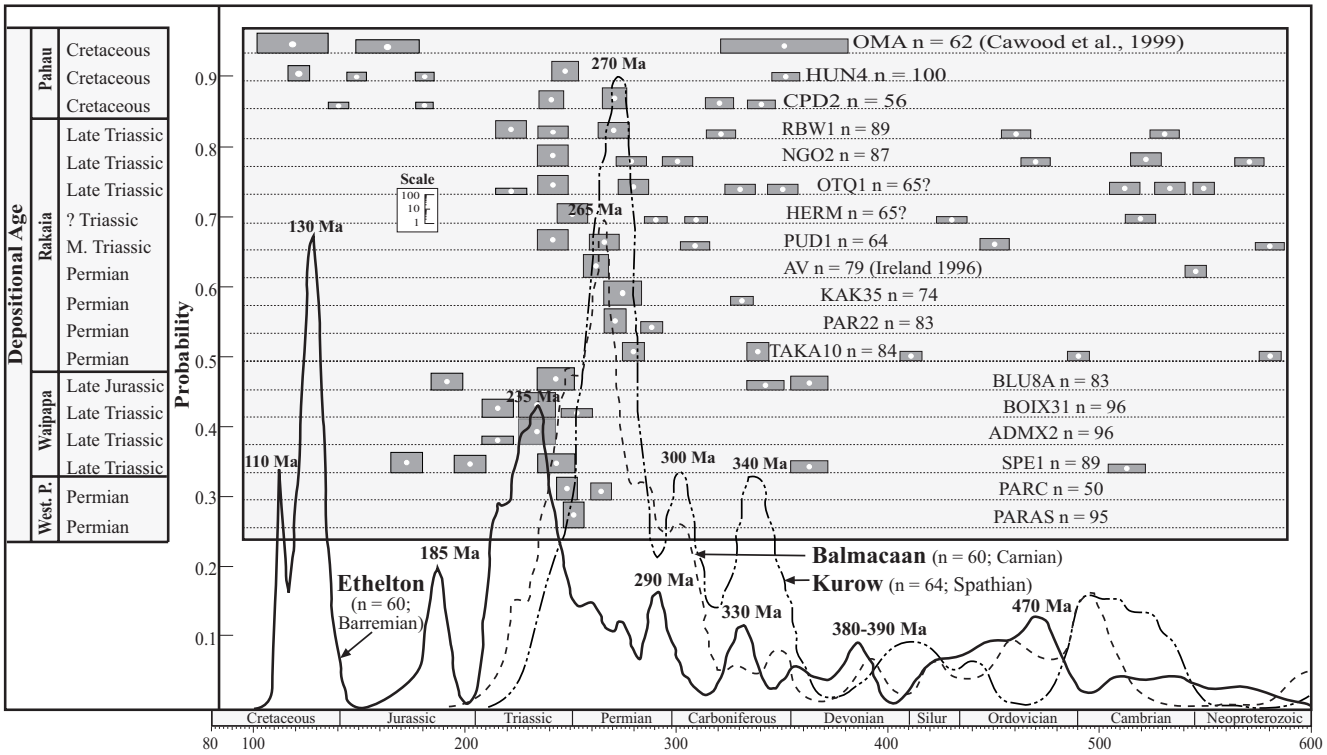

Fig. 8 Cumulative probability distribution curves for the Ethelton Conglomerate matrix and the two Rakaia Terrane sandstones from Kurow and Balmacaan. Detrital zircon age data from Ireland (1992), Wysoczanski et al. (1997), Cawood et al. (1999), and Pickard et al. (2000) are plotted in the light grey shaded box. The dots represent the peaks from cumulative probability curves and the boxes (dark grey) represent, on the horizontal axis, the age range of the major and minor groups, and on the vertical axis, the proportion of these components (as percent on a logarithmic scale). Diagram adapted from Pickard et al. (2000).

Terrane conglomerates (Te Moana, Lake Hill) and Torlesse sandstones of PF1–3 suggest that clasts in the Te Moana and Lake Hill Conglomerates have been derived mainly by autocannibalistic reworking of older Rakaia rocks. The reworking is illustrated by SiO_2/Al_2O_3–Th/Sc ratios in Fig. 6. The presence of cannibalistically recycled, rounded to well rounded, and indurated sandstone clasts in the Permian Te Moana Conglomerate indicates that accretionary processes in the Rakaia Terrane were dominated by burial of sediment and predated the Caples/Torlesse Terrane collision. Induration and exhumation of Torlesse rocks was followed by the erosion and redeposition of the rocks within a short time span.

Uplift of the Rakaia Terrane during the Cretaceous (Adams & Graham 1997; Little et al. 1999) exposed older Rakaia rocks and at the same time rocks of PF3–4 affinities were exposed in the source area, at least for the Mount Saul Conglomerate. This is shown in Fig. 6 where only clasts from this conglomerate plot in the field of PF4. The exposure of volcanogenic inboard rocks is suggested by the wide range of SiO_2/Al_2O_3–Th/Sc ratios in the sandstone clasts from the Ethelton Conglomerate, suggesting that the Ethelton clasts consist of two distinct populations. The majority of Ethelton clasts show a strong affinity with Rakaia sandstones of PF1–3, whereas the clasts with volcanic terrane affinities have some of the highest percent mafic content of all sandstone clasts, and this is reflected in high Sc and low Th concentrations, indicating that sandstones of a more primitive nature were accessible for erosion. There are various mafic source rocks that could have contributed detritus by erosion to the Pahau Basin, including the Brook Street, Murihiku, Maitai, and Caples Terranes. The more mafic Ethelton sandstone clasts show strong petrographic similarities with the felsic Murihiku and Caples Terrane sandstones (MacKinnon 1983, fig. 7, 8). However, if offshore borehole (Waimamaku-2) interpretations by Isaac et al. (1994) are correct (bottom of core interpreted as Murihiku), then the Murihiku Terrane is still a depositional basin (sediment trap) at the time of the Pahau sandstone deposition and cannot be a major contributor of detritus. This problem is resolved by the suggestion of Kear & Mortimer (2003) that subsidence of the Murihiku Basin ceased in the Late Jurassic and an unconformable overlap succession, the Waipa Group, was across the Murihiku and adjacent terranes.

Several lines of evidence presented above and by others strongly support earlier claims (e.g., MacKinnon 1983; Roser & Korsch 1999) that Pahau depocentres received detritus recycled from older Rakaia and Caples Terrane rocks (Roser & Korsch 1999; Wandres et al. 2004b). The recycling is further supported by detrital zircon data (Fig. 8). The two Rakaia Terrane samples analysed each contain a major age group in the range of 360–220 Ma (Middle Triassic–Devonian) that comprise 51 and 70%, respectively, of the dataset. The major peak of the Permian Kurow sample is at c. 270 Ma, indistinguishable from other published Permian Rakaia sandstones. The early Late Triassic (Carnian) Balmacaan Stream detrital zircon age distribution agrees well with a Middle Triassic sample analysed nearby (PUD1, Pickard et al. 2000) with a slightly older main peak at 265 Ma.

The major age group of the Lower Cretaceous (Barremian) Ethelton matrix sample makes up 38% of the sample dataset,

and this group is indistinguishable from major age groups recognised in Triassic Rakaia, Waipapa/Caples, and Western Province (Parapara Group) sandstones. The peak at c. 235 Ma strongly coincides with peaks recognised in these samples. A second pronounced peak at c. 130 Ma in the Ethelton sample is reflected in sandstone samples from other Pahau localities. Minor peaks at c. 300, 330, and 500 Ma are apparent in all three sandstone samples and similar peaks are documented from other sandstones from all terranes shown in Fig. 8. The minor peak at c. 180 Ma recognised in the Ethelton sample is also recognised as a minor peak in other Pahau samples from other localities.

The main zircon age group (250–200 Ma) of the Ethelton sandstone is indistinguishable from the Triassic Rakaia and Waipapa/Caples detrital zircon age components. The two minor age groups (300–280 Ma; 340–320 Ma) from Ethelton coincide with Permian and Carboniferous Rakaia components. The minor Ordovician, and the rather subdued Cambrian and Precambrian age components in the Ethelton sample broadly resemble those of both the Rakaia and Waipapa/Caples Terrane rocks, whereas the Devonian peak in the Ethelton sandstone is absent in the older terranes.

The strong correlation between the Triassic peaks from the Ethelton matrix and the inboard terranes lends further strong support to the conclusions obtained from sandstone clast petrography and geochemistry that there was recycling of older Rakaia and Caples rocks into the Pahau depositional basin. The Early Jurassic peaks recognised in the Ethelton matrix (and other Pahau sandstones) and the Waipapa/Caples Terrane coincide with the age of an igneous clast from a Pahau conglomerate (Kekerengu) and the Bounty Island Granite (Wandres et al. 2004b). The peaks also broadly coincide with the proposed docking of the Caples and Rakaia Terranes in the Jurassic and indicate that both the Pahau and the Waipapa/Caples Terranes might have received detritus from a common source of Early Jurassic age.

SUMMARY

We present the first combined detailed information on petrography and geochemistry of Torlesse conglomerate sandstone clasts and use our own and published U-Pb SHRIMP detrital zircon age data to support earlier hypotheses of the recycling of the Rakaia Terrane into the Pahau Terrane. Clast populations in all conglomerates are dominated by indurated to well indurated, rounded to well rounded, immature, moderately sorted, angular feldspathic arenites.

Sandstone clasts from two Rakaia and two Pahau conglomerates were collected to investigate the recycling of the older Rakaia rocks. Sandstone clast major and trace element chemical data largely support petrographic observations derived from thin-section analysis. The similarities of petrographic and geochemical data between sandstone clasts from the Rakaia Terrane and Rakaia sandstones suggest that clasts in the Te Moana and Lake Hill Conglomerates were derived by autocannibalistic reworking of older, consolidated, Rakaia sediments.

Petrography and geochemistry of clasts from the Pahau Terrane suggest that uplift of the Rakaia Terrane continued into the Cretaceous. These Pahau Terrane clasts indicate that at the time of the Pahau sedimentation, Permian to early Late Triassic Rakaia rocks were exposed and recycled into the Pahau Basin across the Esk Head Melange. Recycling of the Rakaia sediments is supported by the detrital zircon age data from this and other studies.

ACKNOWLEDGMENTS

The authors thank Nick Mortimer and Peter Cawood for thorough and critical review, which helped to improve the manuscript. This paper represents part of a PhD thesis by A. M. Wandres funded by a scholarship at the University of Canterbury. The costs of field and laboratory work were partially funded by the Mason Trust and a University of Canterbury research grant.

REFERENCES

Adams CJ, Graham IJ 1996. Metamorphic and tectonic geochronology of the Torlesse terrane, Wellington, New Zealand. New Zealand Journal of Geology and Geophysics 39: 157–180.

Adams CJ, Graham IJ 1997. Age of metamorphism of Otago schist in eastern Otago and determination of protoliths from initial strontium isotope characteristics. New Zealand Journal of Geology and Geophysics 40: 275–286.

Adams CJ, Kelley S 1998. Provenance of Permian-Triassic and Ordovician metagraywacke terranes in New Zealand: evidence from Ar-40/Ar-39 dating of detrital micas. Geological Society of America Bulletin 110: 422–432.

Andrews PB, Speden IG, Bradshaw JD 1976. Lithological and paleontological content of the Carboniferous–Jurassic Canterbury Suite, South Island, New Zealand. New Zealand Journal of Geology and Geophysics 19: 791–819.

Barnes PM 1990. Provenance of Cretaceous accretionary wedge sediments: the Mangapokia Formation, Wairarapa, New Zealand. New Zealand Journal of Geology and Geophysics 33: 125–135.

Bhatia MR, Crook KAW 1986. Trace element characteristics of greywackes and tectonic setting discrimination of sedimentary basins. Contributions to Mineralogy and Petrology 92: 181–193.

Bradshaw JD 1973. Allochthonous Mesozoic fossil localities in melange in the Torlesse Group of North Canterbury. Journal of the Royal Society of New Zealand 3: 161–167.

Bradshaw JD 1989. Cretaceous geotectonic pattern in the New Zealand Region. Tectonics 8: 803–820.

Bradshaw JD, Adams CJ, Andrews PB 1981. Carboniferous to Cretaceous on the Pacific margin of Gondwana; the Rangitata phase of New Zealand. In: Cresswell M, Vella P ed. Gondwana five. Rotterdam, AA Balkema. Pp. 217–221.

Campbell JD, Warren G 1965. Fossil localities of the Torlesse group in the South Island. Transactions of the Royal Society of New Zealand, Geology 3: 99–137.

Cawood PA, Nemchin AA, Leverenz A, Saeed A, Ballance PF 1999. U/Pb dating of detrital zircons: implications for the provenance record of Gondwana margin terranes. Geological Society of America Bulletin 111: 1107–1119.

Cawood PA, Landis CA, Nemchin AA, Hada S 2002. Permian fragmentation, accretion and subsequent translation of a low-latitude Tethyan seamount to the high-latitude East Gondwana margin; evidence from detrital zircon age data. Geological Magazine 139: 131–144.

Coombs DS, Landis CA, Norris RJ, Sinton JM, Borns DJ, Craw D 1976. The Dun Mountain Ophiolite Belt, New Zealand, its tectonic setting, constitution and origin, with special reference to the southern portion. American Journal of Sciences 276: 561–603.

Dickinson WR 1970. Interpreting detrital modes of greywacke and arkose. Journal of Sedimentary Petrology 40: 695–707.

Dickinson WR, Beard LS, Brakenridge GR, Erjavec JL, Ferguson RJ, Inman KF, Knepp RA, Lindberg FA, Ryberg PT 1983. Provenance of North American Phanerozoic sandstones in relation to tectonic setting. Geological Society of America Bulletin 94: 222–235.

Fedo CM, Nesbitt HW, Young GM 1995. Unraveling the effects of potassium metasomatism in sedimentary rocks and paleosols, with implications for paleoweathering conditions and provenance. Geology 23: 921–924.

Frost CD, Coombs DS 1989. Nd isotope character of New Zealand sediments: implications for terrane concepts and crustal evolution. American Journal of Science 289: 744–770.

George AD 1992. Deposition and deformation of an Early Cretaceous trench-slope basin deposit, Torlesse terrane, New Zealand. Geological Society of America Bulletin 104: 570–580.

Howell DG 1980. Mesozoic accretion of exotic terranes along the New Zealand segment of Gondwanaland. Geology 8: 487–491.

Ingersoll RV, Suczek CA 1979. Petrology and provenance of Neogene sand from Nicobar and Bengal Fans, DSDP sites 211 and 218. Journal of Sedimentary Petrology 49: 1217–1228.

Ireland TR 1992. Crustal evolution of New Zealand: evidence from age distributions of detrital zircons in Western Province paragneisses and Torlesse greywacke. Geochimica et Cosmochimica Acta 56: 911–920.

Isaac MJ, Herzer RH, Brook FJ, Hayward BW 1994. Cretaceous and Cenozoic sedimentary basins of Northland, New Zealand. Institute of Geological & Nuclear Sciences Monograph 8. Lower Hutt, New Zealand, Institute of Geological & Nuclear Sciences Ltd. 204 p.

Jones PJ 1995. AGSO Phanerozoic timescale: wallchart and explanatory notes. Melbourne, Australia, Oxford University Press. 32 p.

Kear D, Mortimer N 2003. Waipa Supergroup, New Zealand: a proposal. Journal of the Royal Society of New Zealand 33: 149–163.

Korsch RJ, Wellman HW 1988. The geological evolution of New Zealand and the New Zealand region. In: Nairn AEM, Stehli FG, Uyeda S ed. The oceanic basins and margins. Vol. 7B: The Pacific Ocean. New York, Plenum Press. Pp. 411–482.

Kroonenburg SB 1994. Effect of provenance, sorting and weathering on the geochemistry of fluvial sand from different tectonic and climatic environments. Proceedings of the 29th International Geological Congress, Part A. Pp. 69–81.

Le Maitre RW 1976. The chemical variability of some common igneous rocks. Journal of Petrology 17: 589–637.

Leverenz A, Ballance PF 2001. Terrane affiliation and terrane boundaries of Mesozoic accretionary complexes, northeastern North Island, New Zealand: some implications from recycling. New Zealand Journal of Geology and Geophysics 44: 589–599.

Little TA, Mortimer N, McWilliams M 1999. An episodic Cretaceous cooling model for the Otago-Marlborough Schist, New Zealand, based on Ar-40/Ar-39 white mica ages. New Zealand Journal of Geology and Geophysics 42: 305–325.

MacKinnon TC 1980. Sedimentologic, petrographic, and tectonic aspects of Torlesse and related rocks: Unpublished PhD thesis, University of Otago, Dunedin, New Zealand.

MacKinnon T 1983. Origin of the Torlesse terrane and coeval rocks, South Island, New Zealand. Geological Society of America Bulletin 94: 967–985.

McLennan SM, Hemming S, McDaniel DK, Hanson GN 1993. Geochemical approaches to sedimentation, provenance, and tectonics. In: Johnsson MJ, Basu A ed. Processes controlling the composition of clastic sediments. Special paper, Geological Society of America. Boulder, CO, Geological Society of America (GSA). Pp. 21–40.

Mazengarb C, Harris DHM 1994. Cretaceous stratigraphic and structural relations of the Raukumara Peninsula, New Zealand: stratigraphic patterns associated the migration of a thrust system. Annales Tectonicae VIII: 100–118.

Mortimer N 1993. Jurassic tectonic history of the Otago Schist, New Zealand. Tectonics 12: 237–244.

Mortimer N 1995. Origin of the Torlesse terrane and coeval rocks, North Island, New Zealand. International Geology Review 36: 891–921.

Muir RJ, Ireland TR, Weaver SD, Bradshaw JD, Waight TE, Jongens R, Eby GN 1997. SHRIMP U-Pb geochronology of Cretaceous magmatism in northwest Nelson-Westland, South Island, New Zealand. New Zealand Journal of Geology and Geophysics 40: 453–463.

Nesbitt HW, Young GM 1982. Early Proterozoic climates and plate motions inferred from major element chemistry of lutites. Nature (London) 299: 715–717.

Pickard AL, Adams CJ, Barley ME 2000. Provenance of New Zealand Late Permian to Cretaceous depocentres at the Australian margin of Gondwanaland: evidence from detrital zircon SHRIMP dating. Australian Journal of Earth Sciences 47: 987–1007.

Roser BP 1986. Chemistry, provenance and tectonic setting of New Zealand greywacke terranes. Geological Society of New Zealand 16th annual conference; programme and abstracts. Christchurch, Geological Society of New Zealand. 88 p.

Roser BP, Korsch RJ 1986. Determination of tectonic setting of sandstone-mudstone suites using SiO_2 content and K_2O/Na_2O ratio. The Journal of Geology 94: 635–650.

Roser BP, Korsch RJ 1988. Provenance signatures of sandstone-mudstone suites determined using discriminant function analysis of major-element data. Chemical Geology 67: 119–139.

Roser BP, Korsch RJ 1999. Geochemical characterization, evolution and source of a Mesozoic accretionary wedge: the Torlesse terrane, New Zealand. Geological Magazine 136: 493–512.

Roser BP, Grapes RH, Palmer K 1993. Petrofacies and subterrane affiliation of Torlesse sediments, southern North Island, New Zealand. Geological Society of New Zealand Miscellaneous Publication 79A. 130 p.

Roser BP, Grapes RH, Palmer K 1995. XRF analyses of sandstones and argillites from the Torlesse terrane, New Zealand. Geology Board of Studies Publication 15. Wellington, New Zealand, Victoria University of Wellington Geology Board of Studies. 40 p.

Silberling NJ, Nichols KM, Bradshaw JD, Blome CD 1988. Limestone and chert in tectonic blocks from the Esk Head subterrane, South Island, New Zealand. Geological Society of America Bulletin 100: 1213–1223.

Smale D 1978. The composition of a Torlesse conglomerate: Ethelton, North Canterbury. New Zealand Journal of Geology and Geophysics 21: 699–711.

Smale D 1980. Akatarawa Conglomerate (Permian), Lake Aviemore, South Canterbury. New Zealand Journal of Geology and Geophysics 23: 279–292.

Smale D 1983. The Te Moana Conglomerate (Torlesse), Four Peaks Range, South Canterbury. New Zealand Journal of Geology and Geophysics 26: 259–270.

Smale D 1997. Heavy minerals in the Torlesse terrane of the Wellington area, New Zealand. New Zealand Journal of Geology and Geophysics 40: 499–506.

Taylor SR, McLennan SM 1985. The continental crust: its composition and evolution. Oxford, Blackwell Scientific. 312 p.

Van Der Plas L, Tobi AC 1965. A chart of judging the reliability of point counting results. American Journal of Science 263: 87–90.

Van Dusschoten A 1998. Balmacaan Stream; a significant Middle Triassic Torlesse fossil locality in mid Canterbury. Geological Society of New Zealand Miscellaneous Publication 101A: 235.

Wandres AM, Bradshaw JD 2005. New Zealand tectonostratigraphy and implications from conglomeratic rocks for the configuration of the SW Pacific of Gondwana. In: Vaughan APM, Leat PT, Pankhurst R ed. Terrane processes at the margin of Gondwana. Journal of the Geological Society London Special Publication: 246: 179–206.

Wandres AM, Bradshaw JD, Weaver SD, Maas R, Ireland TR, Eby GN 2004a. Provenance of the sedimentary Rakaia terrane, Torlesse Terrane, South Island, New Zealand: the use of igneous clast compositions to define the source. Sedimentary Geology 168: 193–226.

Wandres AMC, Bradshaw JD, Weaver SD, Maas R, Ireland TR, Eby GN 2004b. Provenance analysis using conglomerate clast lithologies: a case study from the Pahau Terrane of New Zealand. Sedimentary Geology 167: 57–89.

Weaver SD, Gibson IL, Houghton BF, Wilson CJ 1990. Mobility of rare earth and other elements during crystallisation of alkaline silicic lavas. Journal of Volcanology and Geothermal Research 43: 57–70.

Wysoczanski RJ, Gibson GM, Ireland TR 1997. Detrital zircon age patterns and provenance in Late Paleozoic Early Mesozoic New Zealand; terranes and development of the Paleo-Pacific Gondwana margin. Geology 25: 939–942.